

See discussions, stats, and author profiles for this publication at: <https://www.researchgate.net/publication/50990306>

Facile C–S coupling reaction of aryl iodide and thiophenol catalyzed by Cu-grafted furfural functionalized mesoporous organosilica

ARTICLE *in* DALTON TRANSACTIONS · APRIL 2011

Impact Factor: 4.2 · DOI: 10.1039/c0dt01771j · Source: PubMed

CITATIONS

27

READS

59

4 AUTHORS:



John Mondal

Indian Institute of Chemical Technology

34 PUBLICATIONS 706 CITATIONS

SEE PROFILE



Arindam Modak

Indian Association for the Cultivation of Sci...

26 PUBLICATIONS 556 CITATIONS

SEE PROFILE



Arghya Dutta

RIKEN

32 PUBLICATIONS 499 CITATIONS

SEE PROFILE



Asim Bhaumik

Indian Association for the Cultivation of Sci...

294 PUBLICATIONS 4,651 CITATIONS

SEE PROFILE

Facile C–S coupling reaction of aryl iodide and thiophenol catalyzed by Cu-grafted furfural functionalized mesoporous organosilica

John Mondal, Arindam Modak, Arghya Dutta and Asim Bhaumik*

Received 15th December 2010, Accepted 4th March 2011

DOI: 10.1039/c0dt01771j

A new functionalized mesoporous organosilica has been designed *via* Schiff-base condensation of furfural and 3-aminopropyltriethoxy-silane (APTES) followed by its hydrothermal co-condensation with tetraethylorthosilicate (TEOS) in the presence of a cationic surfactant CTAB. Subsequent reaction of this mesoporous organosilica with Cu(OAc)₂ in absolute ethanol leads to the formation of a new Cu(II)-grafted mesoporous organosilica catalyst **1**. Powder XRD, HR TEM, FE SEM, N₂ sorption and FT IR spectroscopic tools are used to characterize the materials. This Cu-anchored mesoporous material acts as an efficient, reusable catalyst in the aryl-sulfur coupling reaction between aryl iodide and thiophenol for the synthesis of value added diarylsulfides.

Introduction

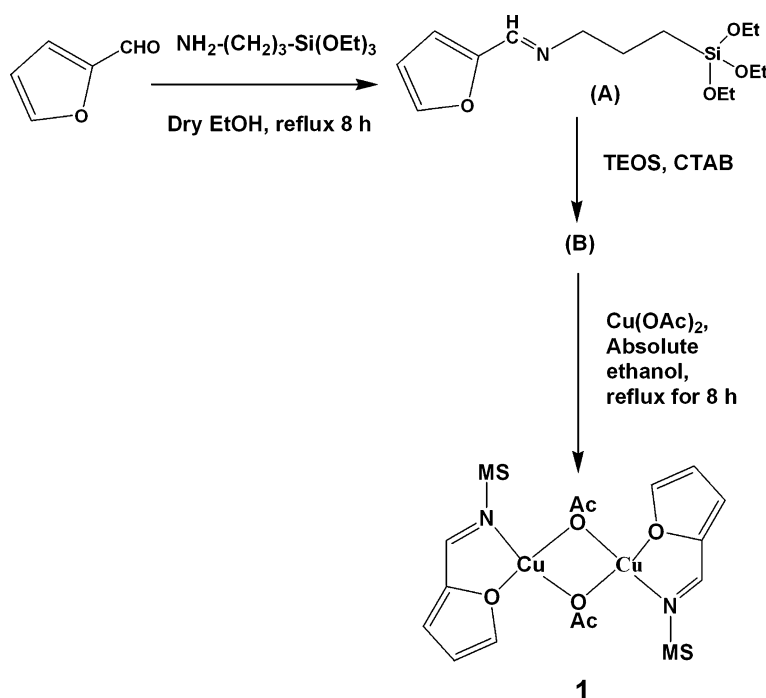
Organically functionalized mesoporous materials have attracted great attention in recent times due to their huge potential applications in gas storage,¹ sensing,² light-harvesting,³ catalysis,⁴ drug-delivery⁵ and so on. For an efficient and reusable catalyst strong binding of the active metal centres to the mesopore surface *via* coordination/covalent bond is very crucial and this can eliminate the possibility of leaching of the active metal from the catalyst surface. Ease of separation of the product from the reaction mixture, recovery of catalyst by simple filtration and excellent recycling efficiency makes the heterogeneous catalysts potentially more useful over their corresponding metal complexes as homogeneous catalysts.⁶ Among different approaches for heterogenization, stabilization/incorporation of an active metal into insoluble zeolitic frameworks,⁷ mesoporous solids,⁸ or related inorganic solids⁹ having high surface areas are considered extensively. Mesoporous organosilica, which offers large pores with a high surface area and donor sites to capture the metal complex, can stabilize the active metal centres under different reaction conditions due to the presence of monodentate, bidentate or tetradentate chelating donor sites at the mesopore surfaces.¹⁰

In this context it is pertinent to mention that C–S, C–N and C–O bond formation reactions offer an indispensable tool for designing new target molecules in synthetic organic chemistry.¹¹ A large variety of aryl-sulfur compounds are used for the treatment of Alzheimer's and Parkinson's disease¹² and also for cancer.¹³ Molecules containing C–S bonds are also used as a molecular precursor for the synthesis of new materials.¹⁴ However, transition metal mediated C(aryl)–S bond formation is less studied than the corresponding C–N and C–O bonds as C–S bond formation is a

very tedious job due to the more favourable parallel oxidative S–S coupling reaction and the simultaneous deactivation of the metal catalyst through the coordination with a sulfur heteroatom.¹⁵ C–S bond formation could proceed *via* the reduction of sulfones and sulfoxides by using strong reducing agents like LiAlH₄.¹⁶ The C–S cross coupling reaction of aryl halides and thiophenol for the development of new C–S bonds is very important industrially as the cost and environmental pollution of the process is relatively low.⁹ Aryl-sulfur coupling reactions can be carried out by using Pd,¹⁷ Fe,¹⁸ Co, Ni and Cu¹⁹ containing homogeneous catalysts carrying suitable ligands. The use of Pd-catalysts in the large-scale processes has been limited due to the high cost of Pd(OAc)₂ and air sensitivity of palladium catalysts. Moreover, the efficient palladium catalysts are usually prepared by using organophosphorous or phosphine ligands, which are difficult to prepare and environmentally unfriendly. A problem arises for the Ni and Co catalysts since these are toxic in nature and have low turnover numbers in their respective reactions. On the other hand, Cu-catalysts are prepared from Cu-salts, which are very cheap and easily available. The problems traditionally associated Cu-mediated reactions include very high temperature, long reaction time, severe reaction conditions and the requirement of greater amount of Cu-salt than its stoichiometry.^{6,20} So a successful strategy for designing an alternative inexpensive, non-air sensitive and recyclable heterogeneous catalyst anchored by Cu-centres on a high surface area material is highly desirable to address these industrial and environmental concerns.

Herein, we report the synthesis of a new furfural functionalized mesoporous organosilica grafted with Cu(II) (Scheme 1, catalyst **1**) and its excellent catalytic activity in the aryl-sulfur coupling reaction of aryl iodide and thiophenol in the presence of a base. Functionalized mesoporous organosilica has been prepared by using the Schiff-base condensation product of furfural and an organic ligand (3-aminopropyl-triethoxysilane) as precursor. The

Department of Materials Science, Indian Association for the Cultivation of Science, Jadavpur 700 032, India. E-mail: msab@iacs.res.in



Scheme 1

material is thoroughly characterized by using powder XRD, HR TEM, FE SEM, N_2 sorption, ICP-AES, UV-vis and FT IR spectroscopic tools. This new mesoporous catalyst remains in a separate solid phase in the reaction mixture, as a result of which the recovery of the catalyst can be easily done by simple filtration and the reaction can proceed without any precaution of inert atmospheric conditions.

Experimental

Synthesis of Schiff base ligand:

A solution of furfural (0.01 mol, 0.9609 g) in dry ethanol (20 mL) was placed under an argon atmosphere in a two neck round bottom flask equipped with a condenser and an additional funnel. A solution of APTES (0.01 mol, 2.21 g, Aldrich) in dry ethanol (5 mL) was added dropwise into the furfural solution over 20 min under continuous stirring conditions. After the complete addition of the organic ligand the reaction mixture was kept under reflux conditions for about 8 h. Then reaction mixture was allowed to cool at room temperature and excess solvent was evaporated to dryness, leaving behind a dark brown coloured viscous gel. This dark brown coloured viscous liquid was designated as **A** and it was characterized by ^1H and ^{13}C NMR.²¹

Synthesis of furfural functionalized mesoporous organic hybrid silica (**B**):

A was used as an organosilane precursor along with tetraethyloxysilicate (TEOS, Aldrich) in 1 : 5 molar ratio for the synthesis of organically functionalized mesoporous silica. Cetyltrimethylammonium bromide (CTAB) was used as a structure directing agent and tartaric acid was used to maintain the initial pH of the solution. In a typical synthesis procedure CTAB (Loba Chemie,

0.0075 mol, 2.73 g) was dissolved in an aqueous solution of tartaric acid (0.6 g in 20 g of H_2O) under vigorous stirring conditions. The resulting mixture was stirred for about 30 min to obtain a clear solution. Then dark brown colour viscous gel (1.35 g) was added dropwise into the surfactant solution under stirring conditions for about 2 h. After 2 h of stirring 5.245 g of TEOS (0.025 mol) was added in the reaction mixture and it was stirred for about 2 h to obtain a gel. After 2 h stirring 2 M NaOH solution was added dropwise into the gel until the pH reached *ca.* 12.0. The resulting gel was kept under stirring for another 12 h at room temperature and then hydrothermally treated at 353 K for 72 h under static conditions. The yellow coloured solid was recovered under filtration, washed several times with water and dried under vacuum. The template CTAB was removed from the as-synthesized sample by extracting the solid three times with an ethanolic solution of HCl at room temperature and this sample is designated as **B**.

Synthesis of mesoporous organic silica supported Cu(II) catalyst (**1**)

1 g of the respective dried mesoporous material grafted with Schiff-base ligand **B** was suspended in an absolute ethanol (20 mL) solution of copper(II) acetate (0.5 g) and was kept under refluxing conditions for about 8 h at 393 K. The colour of the mesoporous material was slowly changed from yellow to light green and no further colour change occurred on further reflux. The reaction mixture was cooled at room temperature and the resulting mesoporous material was filtered through suction with thorough washing with ethanol. After washing it was dried under vacuum. The light green coloured mesoporous material was designated as Cu-grafted catalyst **1**. The outline for the preparation of this furfural functionalized mesoporous silica supported Cu(II) catalyst is shown in Scheme 1.

General procedure for aryl-sulfur coupling reaction of Thiophenol with Aryl iodide:

Cu-grafted furfural functionalized mesoporous silica **1** (Scheme 1) was used as a catalyst for the aryl-sulfur coupling of thiophenol with aryl iodide. To a solution of iodobenzene (204 mg, 1 mmol) and thiophenol (121 mg, 1.1 mmol) in 3 mL of DMF, K_2CO_3 (276 mg, 2 mmol) and Cu-grafted catalyst **1** (20 mg) were added. The mixture was heated at 383 K in a oil bath and the progress of the reaction was monitored by TLC. After a period of time the reaction mixture was allowed to cool and the catalyst was separated by simple filtration. The catalyst was washed and the filtrate was diluted with Et_2O (20 mL) and extracted with Et_2O with the addition of 10% aqueous NaOH solution. The combined organic layer was washed with water and brine solution. Then the combined organic layer was dried over Na_2SO_4 and evaporated to dryness to give the crude product diphenylsulfide as a colourless oil. The isolated crude product was characterized by 1H and ^{13}C NMR, respectively. The aryl-sulfur coupling reaction between thiophenol with aryl iodide over catalyst **1** is shown in the Scheme 2.

Characterization techniques. Powder X-ray diffraction patterns were recorded on a Bruker D-8 Advance SWAX diffractometer operated at 40 kV voltages and 40 mA current. The instrument was calibrated with a standard silicon sample, using Ni-filtered $Cu-K\alpha$ ($\lambda = 0.15406$ nm) radiation. Nitrogen adsorption/desorption isotherms are obtained by using a Bel Japan Inc. Belsorp-HP at 77 K. Prior to gas adsorption, samples are degassed for 4 h at 393 K under high vacuum conditions. A JEOL JEM 6700F field emission scanning electron microscope is used for the determination of the morphology of the particles. FT IR spectra of the samples are recorded using a Nicolet MAGNA-FT IR 750 Spectrometer Series II. UV-vis diffuse reflectance spectra of materials **B** and **1** were obtained by using a Shimadzu UV 2401PC spectrophotometer with an integrating sphere attachment. A $BaSO_4$ pellet was used as the background standard. High resolution transmittance electron microscopic (HR TEM) images were recorded in a Jeol JEM 2010 transmission electron microscope. Cu loading in the sample was estimated by using a Perkin-Elmer Optima 2100 DV Inductive Coupled Plasma Atomic Emission Spectroscopy (ICP-AES). 1H and ^{13}C NMR experiments were carried out on a Bruker DPX-300 NMR spectrometer.

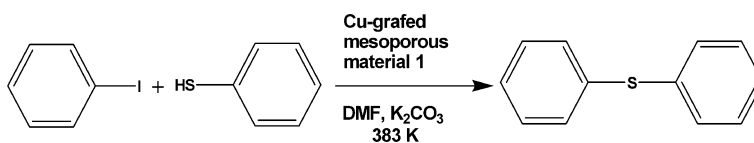
Results and discussion

The small angle X-ray powder diffraction patterns for the as-synthesized and template-extracted samples of **B** are shown in Fig. 1. The as-synthesized sample exhibits a single intense peak with maxima at a 2θ value of 2.58° , attributed to the presence of a disordered mesostructure in the sample. Upon extraction of the sample with an acid-ethanol mixture the intensity of the

Table 1 Unit cell parameters of Cu-loaded catalyst **1**

Phase: Triclinic				
Parameters			Deviations	
$a =$	13.073 Å		0.010	
$b =$	12.289 Å		0.014	
$c =$	10.737 Å		0.006	
$\alpha =$	91.04		0.16	
$\beta =$	91.18		0.13	
$\gamma =$	90.25		0.16	
Unit Cell Volume = 1724.411 Å ³				
ESD = 2.631				
h	k	l	2θ	d
1	0	0	6.77	13.067
0	0	1	8.23	10.727
2	0	0	13.54	6.533
0	2	0	14.46	6.139
2	0	1	16.01	5.527
0	0	3	24.88	3.576
1	0	-3	25.66	3.468
3	1	-2	27.05	3.294
4	0	-1	28.38	3.144
0	4	-1	30.10	2.962
2	4	0	32.25	2.770
2	0	4	36.48	2.462
1	-5	1	38.05	2.362
1	-4	-3	39.40	2.286

peak was reduced and it shifted towards high angle, having a 2θ value of 2.79° , which indicates that the organic template was removed from the as-synthesized material. The d spacing of the mesophase (pore centre to pore centre correlation length) for the as-synthesized (a) and extracted materials (b) are 3.33 nm and 3.12 nm respectively. The d spacing has been reduced in the case of the extracted sample on removal of the template, which suggests a contraction of the pore width after extraction, which is an usual trend for the mesoporous materials. When copper was loaded in the mesoporous hybrid material the small angle peak drastically reduced but an intense peak emerged at a higher value of 2θ , namely 6.89° and 8.38° , respectively (Fig. 1). The wide angle XRD pattern of the Cu-grafted sample is shown in Fig. 2. This powder diffraction peaks can be assigned very well with a new triclinic phase having the following unit cell parameters: $a = 13.073$ Å, $b = 12.289$ Å, $c = 10.737$ Å; $\alpha = 91.04^\circ$, $\beta = 91.18^\circ$ and $\gamma = 90.25^\circ$. The unit cell volume for this triclinic Cu-grafted catalyst **1** is $V = 1724.411$ Å³ and hkl for different planes and the respective d spacings are given in Table 1. The PXRD pattern of the sample has been evaluated with the PXRD pattern calculated by using Reflex, a software package for crystal determination. The CELSIZ program was used to obtain the lattice parameters along with estimated standard deviations (esd, see Table 1). Very small deviations are in accordance with a good fit of the calculated values with the experimental data.



Scheme 2

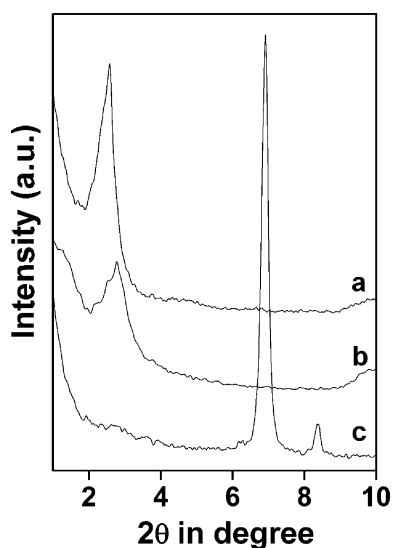


Fig. 1 Small angle powder XRD pattern of the as-synthesized (a) and acid extracted (b) furfural functionalized mesoporous material and the Cu-grafted catalyst **1** (c).

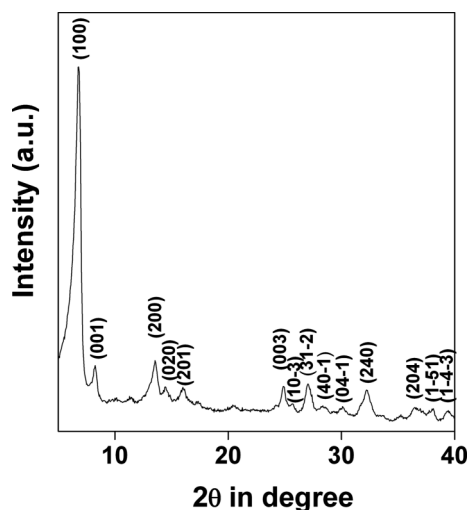


Fig. 2 Wide angle powder XRD pattern of the Cu-grafted catalyst **1**. Different planes are indexed.

N_2 adsorption/desorption isotherms of the mesoporous functionalized silica and Cu-grafted samples are shown in Fig. 3. For clarity the Y axis values of the extracted sample (b) have been multiplied by 2. Both the samples showed a typical type IV isotherm characteristic of mesoporous materials.²² The BET surface area for the extracted and Cu-grafted samples are $617 \text{ m}^2 \text{ g}^{-1}$ and $132 \text{ m}^2 \text{ g}^{-1}$, respectively, with corresponding pore volumes of 0.597 cc g^{-1} and 0.1629 cc g^{-1} , respectively. A considerable decrease in the BET surface area and pore volume suggests that Cu-centres have been anchored on the inner surface of the pores. The pore size distribution of both the samples are calculated by using non-local density functional theory (NLDFT) method shown in the inset of Fig. 3, suggests a uniform distribution of mesopores throughout the samples with pore dimensions of *ca.* 2.5 nm and 2.17 nm, respectively, for sample **B** and catalyst **1**. The calculated pore volume and pore size of the Cu-loaded mesoporous organic hybrid silica is adequate to carry out the aryl-sulfur coupling reaction.

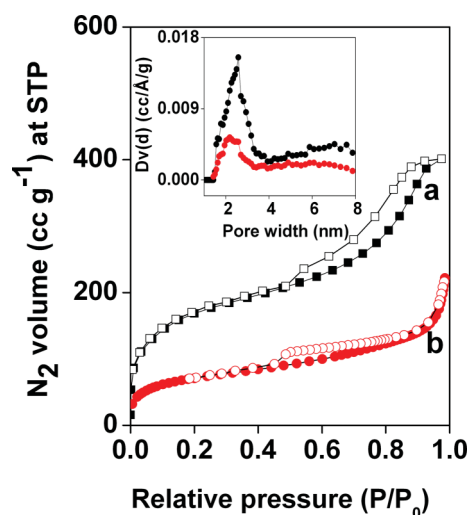


Fig. 3 N_2 adsorption/desorption isotherm of the furfural functionalized mesoporous material (a) and Cu-grafted catalyst **1** (b). Respective pore size distributions, estimated through NLDFT method, are shown in the inset.

The FE SEM image of the sample **B** (a) and Cu-grafted catalyst **1** (b) are shown in Fig. 4. The as-synthesized sample has spherical morphology having dimension *ca.* 120–130 nm and these spherical particles are self-assembled to form large agglomerates. On the other hand the SEM image of the catalyst **1** suggests that the material has rod shaped particle morphology corresponding to a crystalline material. The change from an amorphous to a crystalline structure on Cu-grafting, as observed from the powder XRD results, is clearly observed from this change in particle morphology. The high-resolution TEM images of the Cu-grafted

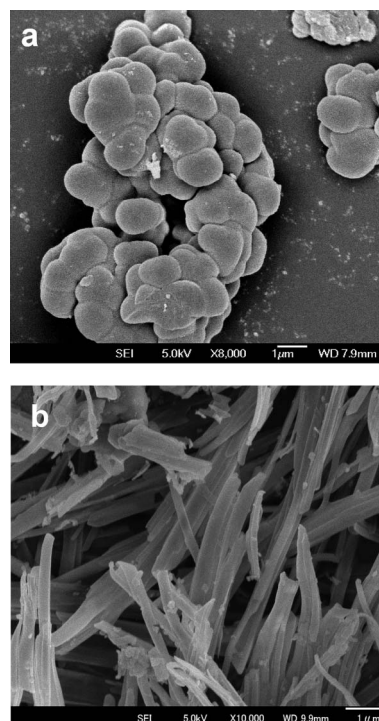


Fig. 4 FE SEM image of the furfural functionalized mesoporous material (a) and Cu-grafted catalyst **1** (b).

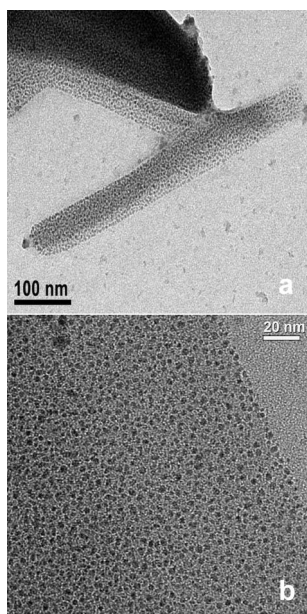


Fig. 5 TEM image of the Cu-grafted catalyst **1** in low (a) and high (b) magnification.

catalyst **1** are shown in Fig. 5. It is clear from this figure that the material is composed of particles having rod shaped morphology. The high magnification image further suggested the existence of pores of dimension 2.2–2.5 nm randomly distributed throughout the material **1**. This result agrees well with the dimension of pores obtained from the N_2 sorption data. Here the change in particle morphology during the grafting of Cu could be attributed to the formation of crystalline Cu-complex at the surface of the mesopores. This is reflected in the powder XRD pattern of material **1** also. Thus, the change in morphology is due to phase change (amorphous to triclinic structure) during Cu-grafting and the origin of reflections belongs to the Cu-complex. The fine particles (dark spots) observed in the TEM image are neither Cu, Cu-oxides or related to silica. It could be attributed to the Cu-nanoclusters formed at the surface of the mesopores due to the network formed on coordination (chelating sites) of imine-N and furfural-O donor sites with Cu. Interestingly, as seen from the TEM image these dark contrast nanocluster/nanoparticle like species are uniformly distributed at the mouth of the mesopores, having dimensions of *ca.* 2–3 nm. Such uniformly distributed fine nanoclusters of the metal-complex could be responsible for the high catalytic activity of this functionalized mesoporous material in the C–S coupling reaction.

The FT IR spectra of the extracted sample (b) and Cu-grafted catalyst (c) are shown in Fig. 6, from which it is evident that the peak at 1637 cm^{-1} for (a) is for $C=N$. For the Cu anchored mesoporous material the $C=N$ stretching frequency is shifted to lower wavelength at *ca.* 1627 cm^{-1} indicating the $C=N$ bond is coordinated to copper through the lone pair of electrons of nitrogen. The two strong absorption bands at 1555 cm^{-1} ²³ and 1436 cm^{-1} ²⁴ can be assigned to the asymmetric and symmetric vibrations, respectively, of the bridging acetate ions and a weak peak at 418 cm^{-1} is attributed to the Cu–N coordination.²⁵ Thus, the presence of these two strong absorption bands at 1555 cm^{-1} and 1436 cm^{-1} in the Cu-grafted furfural functionalized mesoporous

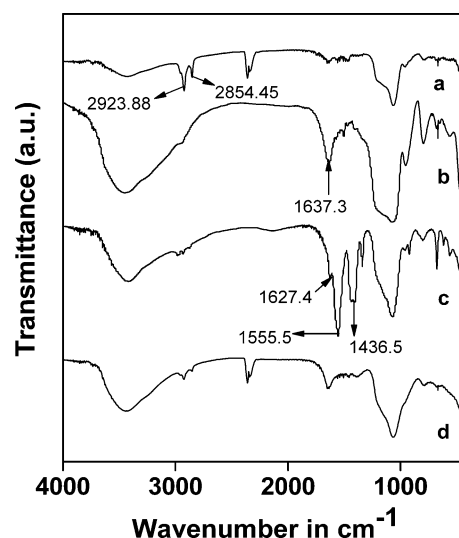


Fig. 6 FT-IR spectra of the furfural functionalized mesoporous material (as-synthesized) (a), extracted material (b), Cu-grafted catalyst **1** (c) and Cu-grafted catalyst after addition of base (d).

material suggested the presence of bridging acetate ions (Scheme 1, **1**). Further, the FT IR spectrum for the as-synthesized sample (Fig. 6a) showed two absorption bands at 2924 cm^{-1} and 2854 cm^{-1} . These could be attributed to the C–H vibrations of the CTAB molecules. But these two strong absorption bands are almost absent in the acid-extracted sample **B**, as shown in Fig. 6b. Thus the FT IR spectral analysis revealed that the template CTAB molecule has been removed almost completely from the as synthesized sample. The UV spectra of the extracted (a) and Cu-loaded (b) samples are given in Fig. 7. In the case of the extracted sample the peak in between 300–400 nm is due to the $\pi-\pi^*$ transition of the conjugated system present in the imine ligand. In the case of the Cu-loaded sample a small hump at around 340 nm is present and a strong peak that arises around 256 nm can be attributed to the charge transfer band between Cu^{+2} and the oxygen of the ligand.²⁶ In addition to this, a very broad absorption band in between 600–800 nm is observed. This

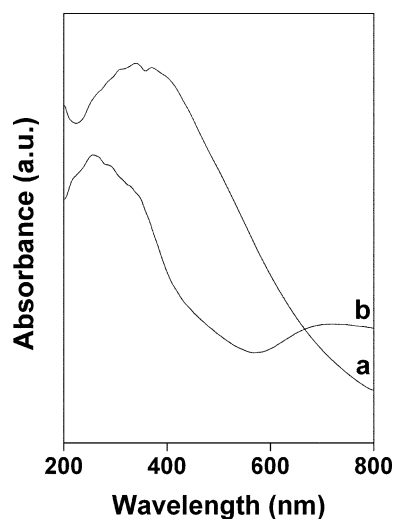


Fig. 7 UV-vis diffuse reflectance spectra of furfural functionalized mesoporous material (a) and Cu-grafted catalyst **1** (b).

could be attributed to the d–d transition of Cu^{+2} ions in a pseudo-octahedral environment.²⁷

Catalysis

The high catalytic activity of different Cu-loaded catalysts^{28,29} has motivated us to explore the possibility of using catalyst **1** in the C–S coupling reaction of various electron-withdrawing and electron-donating aryl iodides. The yields of the different product diarylsulfides obtained in these reactions are high as shown in Table 2. For both symmetrical as well as unsymmetrical diarylsulfides the yield varied from 75–88%.³⁰ The catalytic activity of the Cu-anchored mesoporous material **1** was studied both at elevated temperature (383 K) as well as at room temperature (298 K). As seen from the table, the Cu-grafted furfural functionalized mesoporous organosilica catalyst is highly reactive at elevated temperature and it takes only 7–9 h for the completion of the reaction, whereas at room temperature the yield of the C–S coupling product was 35.2% only (Table 2, entry 6). When we have carried out the coupling reaction of iodobenzene and thiophenol in the presence of Schiff base material **B**, before Cu-grafting and in the absence of any catalyst at 383 K, in both cases not even a trace of the C–S coupling product was observed. On the other hand, in a control experiment when homogeneous phase $\text{Cu}(\text{OAc})_2$ was used as the catalyst under optimized conditions at 383 K only a 20.0% yield of the diphenylsulfide (Table 2, entry 5) was obtained. In Table 2 we have summarized the TOFs for the synthesis of diarylsulfides over catalyst **1**. As seen from the table, for catalyst **1** these TOFs are quite high (varies between 121–183) compared to that of the homogeneous counterpart (copper acetate, TOF = 36.3). The coupling reaction between iodobenzene and thiophenol was also taken as a representative case to check the recycling efficiency of the Cu anchored catalyst. It was found that the catalyst can be efficiently recycled and reused for five repeating cycles without significant loss of catalytic activity. The Cu content in the fresh catalyst and the catalyst obtained after fifth cycle was estimated by ICP-AES. Cu content in the fresh catalyst is 0.68 mmol L^{-1} , whereas for the recovered catalyst after fifth catalytic cycle it is 0.67 mmol L^{-1} . The yield of the product and the Cu content of the catalyst has been marginally reduced after the fifth repetitive catalytic cycle. We have plotted the recycling efficiency of the catalyst for five consecutive catalytic cycles for the coupling reaction of iodobenzene and thiophenol, which is shown in Fig. 8.

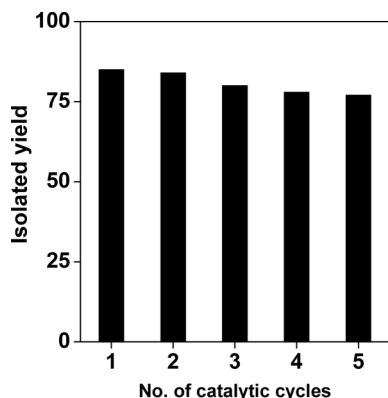


Fig. 8 Recycling efficiency of the Cu-grafted catalyst **1**.

This result suggests that our novel Cu-grafted catalyst is a very efficient catalyst in the C–S coupling reaction.

To test any leaching of the copper into the reaction mixture during the catalytic reactions a hot filtration test was conducted taking the coupling reaction between iodobenzene and thiophenol as a representative case. In this technique, the reaction mixture was filtered under hot condition from the suspended catalyst after 4 h of the reaction and with the filtrate the reaction was continued at the same temperature and for another 4 h. It was observed that there was almost no increase in product yield compared to the conversion that took place after 4 h (46.8 and 46.6% yield for before and after hot filtration, respectively). This result suggests that no leaching of Cu occurred during the course of reaction and the catalyst is purely heterogeneous in nature. A probable mechanistic reaction pathway is suggested in Fig. 9. It shows that on addition of base the active species (**I**) is generated due to reduction. In order to prove the presence of active intermediate **I** (Fig. 9) in the catalytic reaction we have performed *in situ* FT IR analysis of the Cu-grafted mesoporous material when base was added into this system. The FT IR spectrum of the sample at this stage is shown in the Fig. 5d, where the two strong absorption bands at 1555 cm^{-1} and 1436 cm^{-1} are absent. This FT IR result thus suggests that in the presence of base the acetate bridges open-up and the active species **I** (Cu^0) was generated during the C–S coupling reaction. This active species undergoes oxidative addition with aryl iodide to give an intermediate (**II**). In the presence of base, thiophenol reacts with (**II**) to afford another intermediate (**III**) which readily undergoes reductive elimination to yield the desired product and the catalyst get regenerated during this process.

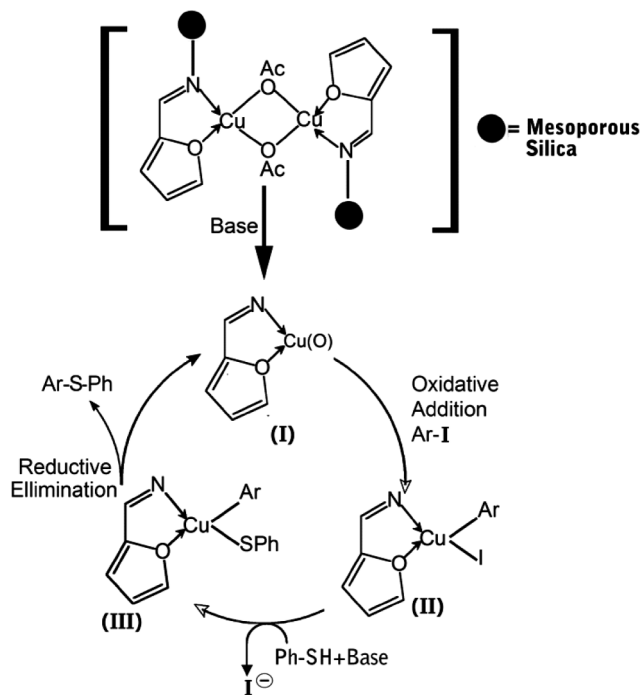
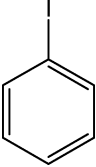
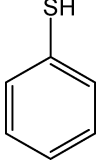
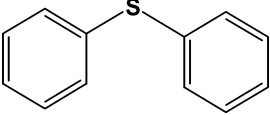
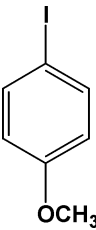
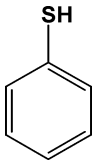
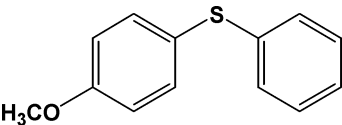
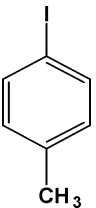
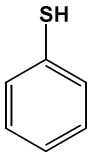
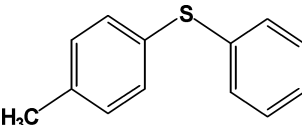
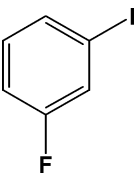
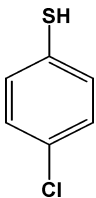
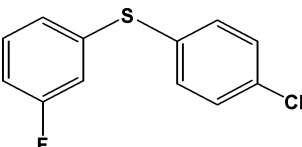
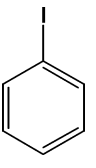
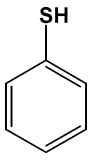
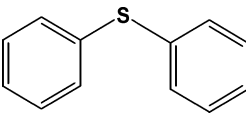
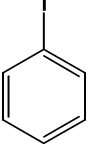
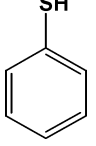
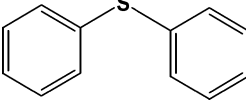


Fig. 9 Catalytic cycle for the C–S coupling reaction.

Conclusions

We have developed a furfural functionalized mesoporous silica material and grafted it with $\text{Cu}(\text{II})$ to obtain a new and robust

Table 2 C–S coupling reactions over Cu-grafted functionalized mesoporous material **1**

Entry	ArI	ArSH	Product (Ar–S–Ar)	Time (h)	Yield (%)	TOF ^a (h ^{−1})
1				8	85.2	154.5
2				7	88.0	182.8
3				7	87.1	180.7
4				9	75.0	121.1
5 ^b				8	20.0	36.3
6 ^c				8	35.2	44.0

^a TOF = Turn over frequency = moles of substrate converted per mole of Cu per h. ^b Cu(OAc)₂ was used as catalyst. ^c Reaction was carried out at 298 K.

heterogeneous catalyst. Aryl-sulfur coupling reaction takes place very easily under aerobic condition over this Cu-grafted catalyst to obtain different value added symmetrical as well as unsymmetrical bis-thioethers. Good catalytic activity and recycling efficiency in this C–S cross coupling reaction suggests the potential application of this Cu-grafted functionalized mesoporous material for the synthesis of additional organic target molecules. The efficient protocol described for the S-arylation of aromatic thiols with aryl iodides over this Cu-grafted functionalized mesoporous material may open new catalytic pathways for the metal-grafted functionalized mesoporous materials.

Acknowledgements

JM, AM and AD thank CSIR, New Delhi for their respective senior research fellowships.

References

- (a) H. Y. Huang, R. T. Yang, D. Chinn and C. L. Munson, *Ind. Eng. Chem. Res.*, 2003, **42**, 2427; (b) A. C. C. Chang, S. S. C. Chuang, M. Gary and Y. Soong, *Energy Fuels*, 2003, **17**, 468–473; (c) J. C. Hicks, J. H. Drese, D. J. Fauth, M. L. Gray, G. G. Qi and C. W. Jones, *J. Am. Chem. Soc.*, 2008, **130**, 2902.

- 2 (a) R. Metivier, I. Leray, B. Lebeau and B. Valeur, *J. Mater. Chem.*, 2005, **15**, 2965; (b) R. Martinez-Manez and F. Sancenon, *Coord. Chem. Rev.*, 2006, **250**, 3081; (c) K. Sarkar, K. Dhara, M. Nandi, P. Roy, A. Bhaumik and P. Banerjee, *Adv. Funct. Mater.*, 2009, **19**, 223–234; (d) A. Wada, S. Tamaru and M. Ikeda, *J. Am. Chem. Soc.*, 2009, **131**, 5321.
- 3 Y. Maegawa, N. Mizoshita, T. Tani and S. Inagaki, *J. Mater. Chem.*, 2010, **20**, 4399.
- 4 (a) C. Gonzalez-Arellano, A. Corma, M. Iglesias and F. Sanchez, *Eur. J. Inorg. Chem.*, 2008, 1107; (b) D. J. Macquarrie, *Top. Catal.*, 2009, **52**, 1640; (c) K. Sarkar, M. Nandi, M. Islam, M. Mubarak and A. Bhaumik, *Appl. Catal., A*, 2009, **352**, 81.
- 5 M. Vallet-Regi, *Dalton Trans.*, 2006, 5211.
- 6 (a) B. C. Gates, *Chem. Rev.*, 1995, **95**, 511; (b) A. Corma and H. Garcia, *Adv. Synth. Catal.*, 2006, **348**, 1391.
- 7 (a) W. B. Fan, R. G. Duan, T. Yokoi, P. Wu, Y. Kubota and T. Tatsumi, *J. Am. Chem. Soc.*, 2008, **130**, 10150; (b) W. Fan, Y. Kubota and T. Tatsumi, *ChemSusChem*, 2008, **1**, 175; (c) M. Sasidharan and A. Bhaumik, *J. Mol. Catal. A: Chem.*, 2010, **328**, 60.
- 8 (a) M. Masteri-Farahani, F. Farzaneh and M. Ghandi, *J. Mol. Catal. A: Chem.*, 2003, **192**, 103; (b) L. Zhang, H. C. L. Abbenhuis, G. Gerritsen, N. Ni Bhriain, P. C. M. M. Magusin, B. Mezari, W. Han, R. A. van Santen, Q. H. Yang and C. Li, *Chem.–Eur. J.*, 2007, **13**, 1210; (c) S. K. Maiti, S. Dinda, M. Nandi, R. G. Bhattacharyya and A. Bhaumik, *J. Mol. Catal. A: Chem.*, 2008, **287**, 135.
- 9 A. Choplin and F. Quignard, *Coord. Chem. Rev.*, 1998, **178**, 1679.
- 10 (a) D. Trong On, D. D. Giscard, C. Danumah and S. Kaliaguine, *Appl. Catal., A*, 2001, **222**, 299; (b) M. H. Valkenberg and W. F. Holderich, *Catal. Rev. Sci. Eng.*, 2002, **44**, 321; (c) C. Baleizao, B. Gigante, M. Sabater, H. Garcia and A. Corma, *Appl. Catal., A*, 2002, **228**, 279; (d) S. L. Jain, B. S. Rana, B. Singh, A. K. Sinha, A. Bhaumik, M. Nandi and B. Sain, *Green Chem.*, 2010, **12**, 374–377.
- 11 D. J. Procter, *J. Chem. Soc., Perkin Trans. 1*, 2001, 335.
- 12 (a) Y. Wang, S. Chackalamannil, Z. Hu, J. W. Clader, W. Greenlee, W. Billard, H. Binch, G. Crosby, V. Ruperto, R. A. Duffy, R. McQuade and J. E. Lachowicz, *Bioorg. Med. Chem. Lett.*, 2000, **10**, 2247; (b) S. F. Nielsen, E. O. Nielsen, G. M. Olsen, T. Liljefors and D. Peters, *J. Med. Chem.*, 2000, **43**, 2217.
- 13 G. De Martino, M. C. Edler, G. La Regina, A. Coluccia, M. C. Barbera, D. Barrow, R. I. Nicholson, G. Chiosis, A. Brancale, E. Hamel, M. Artico and R. Silvestri, *J. Med. Chem.*, 2006, **49**, 947.
- 14 (a) J. F. Hartwig, *Angew. Chem., Int. Ed.*, 1998, **37**, 2046; (b) J. P. Wolfe, S. Wagaw, J. F. Marcoux and S. L. Buchwald, *Acc. Chem. Res.*, 1998, **31**, 805.
- 15 T. Kondo and T. A. Mitsudo, *Chem. Rev.*, 2000, **100**, 3205.
- 16 (a) J. Lindley, *Tetrahedron*, 1984, **40**, 1433; (b) T. Yamamoto and Y. Sekine, *Can. J. Chem.*, 1984, **62**, 1544; (c) R. J. S. Hickman, B. J. Christie, R. W. Guy and T. J. White, *Aust. J. Chem.*, 1985, **38**, 899; (d) A. Van Bierbeek and M. Gingras, *Tetrahedron Lett.*, 1998, **39**, 6283.
- 17 (a) G. Y. Li, G. Zheng and A. F. Noonan, *J. Org. Chem.*, 2001, **66**, 8677; (b) G. Y. Li, *Angew. Chem., Int. Ed.*, 2001, **40**, 1513; (c) U. Schopfer and A. Schlapbach, *Tetrahedron*, 2001, **57**, 3069; (d) T. Itoh and T. Mase, *Org. Lett.*, 2004, **6**, 4587; (e) M. A. Fernandez-Rodriguez, Q. Shen and J. F. Hartwig, *J. Am. Chem. Soc.*, 2006, **128**, 2180.
- 18 (a) A. Correa, M. Carril and C. Bolm, *Angew. Chem., Int. Ed.*, 2008, **47**, 2880; (b) W. Y. Wu, J. C. Wang and F. Y. Tsai, *Green Chem.*, 2009, **11**, 326.
- 19 (a) Y. C. Wong, T. T. Jayanth and C. H. Cheng, *Org. Lett.*, 2006, **8**, 5613; (b) E. Sperotto, G. P. M. van Klink, J. G. de Vries and G. U. Koten, *J. Org. Chem.*, 2008, **73**, 5625; (c) S. Jamm, S. Sakthivel, L. Rout, T. Mukherjee, S. Mandal, R. Mitra, P. Saha and T. Punniyamurthy, *J. Org. Chem.*, 2009, **74**, 1971; (d) H. J. Xu, X. Y. Zhao, J. Deng, Y. Fu and Y. S. Feng, *Tetrahedron Lett.*, 2009, **50**, 434; (e) S. Bhadra, B. Sreedhar and B. C. Ranu, *Adv. Synth. Catal.*, 2009, **351**, 2369.
- 20 (a) J. S. Sawyer, *Tetrahedron*, 2000, **56**, 5045; (b) J. Hassan, M. Sevignon, C. Gozzi, C. Schulz and M. Lemaire, *Chem. Rev.*, 2002, **102**, 1359.
- 21 ¹H NMR (300 MHz, CDCl₃) δ = 7.885 (1H, s), 7.308–7.306 (1H, d), 6.548–6.541 (1H, d), 6.272–6.263 (1H, d), 3.654–3.612 (6H, q), 1.045–1.013 (9H, t), 0.488–0.454 (2H, t), 1.67–1.64 (4H, m). ¹³C NMR (300 MHz, CDCl₃) δ = 151.37, 149.4, 144.19, 111.22, 64.05, 58.0, 18.03, 7.75, 23.91.
- 22 K. Dhara, K. Sarkar, D. Srimani, S. K. Saha, P. Chattopadhyay and A. Bhaumik, *Dalton Trans.*, 2010, **39**, 6395–6402.
- 23 A. Roth, J. Becher, C. Herrmann, H. GoIrls, G. Vaughan, M. Reiher, D. Klemm and W. Plass, *Inorg. Chem.*, 2006, **45**, 10066.
- 24 W. Chen, J. Y. Wang, C. Chen, Qi Yue, H. M. Yuan, J. S. Chen and S. N. Wang, *Inorg. Chem.*, 2003, **42**, 944.
- 25 K. J. Tubbs, A. L. Fuller, B. Bennett, A. M. Arif, M. M. Makowska-Grzyska and L. M. Berreau, *Dalton Trans.*, 2003, 3111.
- 26 M. R. Prasad, G. Kamalakar, S. J. Kulkarni and K. V. Raghavan, *J. Mol. Catal. A: Chem.*, 2002, **186**, 109.
- 27 G. Zhang, J. Long, X. Wang, Z. Zhang, W. Dai, P. Liu, Z. Li, L. Wu and X. Fu, *Langmuir*, 2010, **26**, 1362.
- 28 S. Tanaka, M. Tada and Y. Iwasawa, *J. Catal.*, 2007, **245**, 173.
- 29 P. Roy, M. Nandi, M. Manassero, M. Riccò, M. Mazzani, A. Bhaumik and P. Banerjee, *Dalton Trans.*, 2009, 9543.
- 30 ¹H and ¹³C NMR chemical shifts for different bis-thioethers reported in Table 2: **Entry 1.** ¹H NMR (300 MHz, CDCl₃) δ = 7.519–7.109 (5H, m). ¹³C NMR (300 MHz, CDCl₃) δ = 137.61, 131.17, 129.29, 124.94. **Entry 2.** ¹H NMR (500 MHz, CDCl₃) δ = 3.72 (3H, s); 6.594–6.577 (2H, d), 7.469–7.452 (2H, d), 7.412–7.402 (2H, d), 7.22–7.190 (4H, m), 7.152–7.114 (1H, m). ¹³C NMR (500 MHz, CDCl₃) δ = 159.65, 55.4, 116.53, 138.36, 137.23, 129.21, 127.73, 127.31. **Entry 3.** ¹H NMR (300 MHz, CDCl₃) δ = 2.36 (3H, s), 6.952–6.926 (2H, d), 7.34–7.169 (5H, m). ¹³C NMR (300 MHz, CDCl₃) δ = 21.1, 137.5, 137.18, 132.48, 131.341, 129.934, 127.677, 126.548. **Entry 4.** ¹H NMR (300 MHz, CDCl₃) δ = 7.28 (1H, s), 6.852–6.850 (2H, m), 6.995–6.927 (2H, d), 7.222–7.202 (2H, m). ¹³C NMR (300 MHz, CDCl₃) δ = 113.94, 116.95, 125.5, 129.4, 129.75, 130.5, 132.44, 138.5, 163.0.